

Dynamic Mechanical Properties of Soy Protein Filled Elastomers

L. Jong¹

Dynamic mechanical properties including temperature effect, stress softening, and Payne effect are studied on the elastomer composites filled with soy protein or carbon black. The comparison of protein composite with well-known carbon black composites provides further insight into the protein composites. The elastomers filled with soy protein aggregates give substantial reinforcement effect when compared with the unfilled elastomers. Approximately 400 times increase in shear elastic modulus was observed when 40% by weight of protein is incorporated into the elastomers. The sample films were cast from the particle dispersion of soy protein isolate and carboxylated styrene–butadiene latex. At the higher temperatures, the shear elastic modulus of soy protein-filled composites does not decrease as much as that of the carbon black-filled composites. The behavior of elastic and loss modulus under the oscillatory strain of different magnitude is similar to that of carbon black reinforced styrene–butadiene rubber. However, carbon black composites show a better recovery behavior after eight cycles of dynamic strain. The reduction of shear elastic modulus with dynamic strain (Payne effect) was compared with Kraus model and the fitting parameter related to the aggregate structure of the soy protein. A reasonable agreement between the theoretical model and experiment was obtained, indicating the Payne effect of the protein-related network structure in the elastomers could also be described by the kinetic agglomeration de-agglomeration mechanism.

KEY WORDS: Soy protein; stress softening; Payne effect; rubber composites.

INTRODUCTION

In recent years, many investigations have been made on the modulus enhancement of rubbers by natural materials. Only a few examples are given here [1–3]. From the perspective of renewable materials and environmental reasons, soy protein has been investigated as a component in plastic and adhesive composites [4–8], but has been rarely investigated as a reinforcement component in elastomers. The addition of soy protein to elastomers may improve the biodegradability of rubber composites. However, soy protein also needs to be functional in rubbers. Dry

soy protein is a rigid material and has a shear elastic modulus of ~2 GPa under ambient conditions [5]. Because the high rigidity of a reinforcement phase is one of the requirements in rubber reinforcement, dry protein is therefore a possible candidate for this application. The attempt to use protein in rubber latex can be traced back to 1930's. A few patents [9–11] had claimed the use of protein in rubber composites. For example, Lehmann and coworkers had demonstrated the use of casein (milk protein) in natural rubber latex to achieve approximately four times increase in the modulus [11]. Protein as an additive in rubber materials also has been claimed to improve the anti-skid resistance of winter tread tires [12–14]. In rubber reinforcement, the factors such as aggregate structure, effective filler volume fraction,

¹ United States Department of Agriculture, Agricultural Research Service, National Center for Agricultural Utilization Research, Peoria, IL 61604, USA. E-mail: jong@ncaur.usda.gov

filler–rubber interactions, and elastic modulus of filler clusters have important impact on the modulus of rubber composites [15].

In this study, the rubber matrix chosen is a styrene–butadiene rubber with small amount of carboxylic acid-containing monomer units because previous studies have indicated the importance of interaction between filler and matrix [16]. Soy protein contains a significant amount of carboxylic acid and substituted amine group [17]. Ionic interaction between protein and rubber matrix is therefore possible. Structurally, soy protein is a globule protein and its aggregate is similar to colloidal aggregates. For practical applications, the issue of moisture sensitivity in some applications is always associated with natural materials, but it may be improved through product formulation and/or selective applications. For example, it may be used as a component in multi-layered structures, in coated objects, in elevated temperature applications or as a rubber part in greasy/oily environments where the moisture effect is minimum. The aim of this research is to obtain the information on the structure-properties of soy protein aggregates in rubber composites by analyzing the dynamic mechanical properties.

The rubber composites investigated here are prepared by casting films from soy protein dispersion and a carboxylated styrene–butadiene latex. To give some background on the rubber matrix of this composite, the properties of carboxylated SBR will be described briefly. Carboxylated SBR is classified as an ion-containing polymer where the viscoelastic properties are affected by molecular weight, degree of crosslinking, glass transition temperature (T_g), copolymer composition, the number of ionic functional groups, the size of ionic aggregation, the degree of neutralization, and the size of the neutralizing ions [18, 19]. Previous studies also have shown honeycomb-like structures in the film of carboxylated latexes due to higher concentration of carboxylic acid groups on the particle surface [20]. Mechanically, the elastic modulus of the base rubber is not significant when compared with the modulus of filler network in highly filled elastomeric composites [16]. In this study, a well-known carbon black is used as a comparison because the characteristics of soy protein aggregates are different from that of carbon black in terms of primary particle size in the aggregates, aggregate size, and particle interactions. It is therefore beneficial to use the extensively studied carbon black as a comparison to gain more understanding on the protein composites.

EXPERIMENTAL

Materials and Characterization

The soy protein isolate used in this research is a slightly enzyme-hydrolyzed soy protein isolate (PRO-FAM 781, Archer Daniels Midland Company, Decatur, IL). It contains more than 90% protein, ~6% ash and ~4% fat. Sodium hydroxide, used to adjust pH, is ACS grade. The carboxylated styrene–butadiene (SB) latex is a random copolymer of styrene, butadiene, and small amount of carboxylic acid containing monomers (CP 620NA, Dow Chemical Company, Midland, MI). The glass transition temperature of carboxylated SB Latex is ~10°C determined by differential scanning calorimetry (DSC). Styrene/butadiene ratio estimated from the glass transition temperatures of a series of commercially available carboxylated styrene butadiene is approximately 65/35. The solubility of the dried latex has been tested in our laboratory and the dried latex is not known to be soluble in any solvent or a combination of solvents suggested in the literature [21]. The insolubility of this ionomer excludes the molecular weight and bound rubber measurements. The latex received has ~50% solids and a pH ~6. The pH of the latex is adjusted to 9 before mixing with the protein dispersion. The particle size of the latex is ~0.18 μm . Soy protein isolate was first dispersed in water and the pH was adjusted to 9 with sodium hydroxide. The alkaline soy protein dispersion was then cooked under stirring at 55°C for 60 min to help with the dispersion of the soy protein. After cooking, a homogeneous mixture could be easily obtained by mixing soy protein dispersion with SB latex for about 30 min at ambient temperature due to the low viscosity of the mixture (<0.5 Pa s). After mixing, the pH of mixture was again adjusted to 9. The final aqueous dispersion has 25% solids and 75% water. The composite of soy protein isolate and carboxylated SB latex was prepared by first casting an emulsion of the blend onto an aluminum mold covered with Teflon release sheet (BYTAC from Saint-Gobain Performance Plastics) and then allowing it to dry at 75°C for 72 h. After drying at low temperature, the samples were removed from the mold and annealed at 110°C and 140°C for 24 h, respectively. Dry composites containing 10–40% by weight of soy protein isolate were prepared. The film of 100% carboxylated SB rubber was prepared by adjusting the pH of latex to 9 and dried under the same conditions as that of the Soy/SB composites. Carbon

black (CB) composites were prepared in the same way as the protein composites by mixing an aqueous dispersion of carbon black and styrene-butadiene latex. Aqueous dispersion of carbon black N-339 (Sid Richardson Carbon Co.) was prepared by dispersing carbon black in water with the aid of a surfactant, sodium lignosulfonate (Vanisperse CB, Lignotech USA, Rothschild, WI). The weight fraction of surfactant based on carbon black was 3%. The carbon black does not form a stable dispersion without the aid of surfactant and tends to precipitate due to its higher density (1.73 gm cm^{-3}). The dispersion was homogenized at 10,000 rpm for 1 h. The ~15% carbon black dispersion was then mixed with SB latex and dried in a mold under the same conditions as that of protein composites. The dried carboxylated SBR film contained less than 0.3% moisture and the dried Soy/SB and CB/SB composites had moisture contents less than 0.8% as measured by halogen moisture analyzer (Mettler Toledo HR73) at 105°C for 60 min. For 100% soy protein, a torsion bar could not be made by casting method. The soy protein powder was compression-molded at 47 MPa and 140°C for 2 h. After compression molding, the sample was relaxed at 140°C for 24 h.

Particle Size Measurements

The mean particle size and distribution of carbon black aggregates were measured by using Horiba LA-930 laser scattering particle size analyzer with red light wavelength of 632.8 nm and blue light wavelength of 405 nm. The measurement is based on Mie scattering theory with a measurement range of 0.02–2000 μm . Volume weighted mean diameter of 0.17 μm was obtained for the styrene-butadiene latex, which is in good agreement with particle size data of 0.18 μm supplied by Dow Chemical Company.

Scanning Electron Microscopy

The morphology of the composites and soy protein aggregates were obtained by scanning electron microscopy (SEM) using JEOL JSM-6400 V instrument. The images of soy protein aggregate were obtained by casting onto an aluminum substrate a dilute dispersion of protein at pH 9 and at a concentration of 0.004%. To obtain the images of composites, small pieces of the composite films were fractured under liquid nitrogen and mounted on aluminum stages. The samples on aluminum stages were then coated with a very thin layer of

gold-palladium alloy and the images taken under vacuum at ambient temperature.

Dynamic Mechanical Measurements

For all strain sweep experiments, the oscillatory storage and loss moduli, $G'(\omega)$ and $G''(\omega)$, are measured using a Rheometric ARES-LSM rheometer with a torsional rectangular geometry. A rectangular sample with dimension of approximately $12.5 \times 20 \times 3 \text{ mm}$ was inserted between the top and bottom grips. The gap between the fixtures is 5–6 mm in order to achieve a strain of ~20%. Sample length shorter than 5 mm is not desirable because of the shape change from the clamping at both ends of the sample. The measurement was conducted at 140°C and a frequency of 1 Hz. The oscillatory storage and loss moduli were measured over a strain range of approximately 0.007–20%. The actual strain sweep range is limited by sample geometry and motor compliance at large strain and transducer sensitivity at small strain. Although harmonics in the displacement signal may be expected in non-linear material, a previous study [22] has indicated that the harmonics are not significant if the shearing does not exceed 100%. Each sample was conditioned at 80°C or 140°C for 30 min and then subjected to eight cycles of dynamic strain sweep in order to study the stress softening effect.

Temperature ramp experiments were conducted using torsion rectangular geometry with a heating rate of 1°C/min and a temperature range from –40°C to 140°C. The soak time at each temperature after ramp is 15 s and the measurement duration at each temperature is 30 s. When using torsion rectangular geometry, torsional bars with dimensions of approximately $40 \times 12.5 \times 3 \text{ mm}$ were mounted in the torsion rectangular fixtures and a dynamic mechanical measurement was conducted at a frequency of 0.16 Hz (1 rad s^{-1}) in the linear viscoelastic region.

RESULTS AND DISCUSSION

The Effect of Temperature

As shown in Fig. 1, the addition of soy protein dispersion into styrene-butadiene rubber causes a significant reinforcement effect in the rubber plateau region. The reinforcement effect is proportional to the soy protein content. Soy protein, when dispersed in alkali solution at elevated temperature, hydrolyzes and forms a cloudy but stable dispersion of particle aggregates. The wet soy protein

aggregates in this experiment have particle size in the range of 0.4–12 μm with a surface weighted mean diameter of 2.3 μm and a volume weighted mean diameter of 3.1 μm [23]. The average primary particle size of dry soy protein aggregates was previously determined by scanning electron microscopy (SEM) to be ~ 330 nm [23]. An example of globule soy protein aggregates is shown in Fig. 2. Comparing with soy protein, the primary particle size of carbon black is usually much smaller, typically less than 100 nm, depending on the grade of carbon black. In this particular case, carbon black N339 has a primary particle size of ~ 40 nm. The number and volume averaged size of CB aggregates in the aqueous dispersion is ~ 0.31 μm and ~ 0.62 μm , respectively. The aggregate size of CB aggregates in Fig. 2c is consistent with the number averaged size measured by particle size analyzer. Compared with the soy protein, both primary particle size and aggregate size of carbon black are much smaller. Similar to carbon black particles, soy protein particles may form a network structure, but with stronger inter-particle forces such as hydrogen bonding

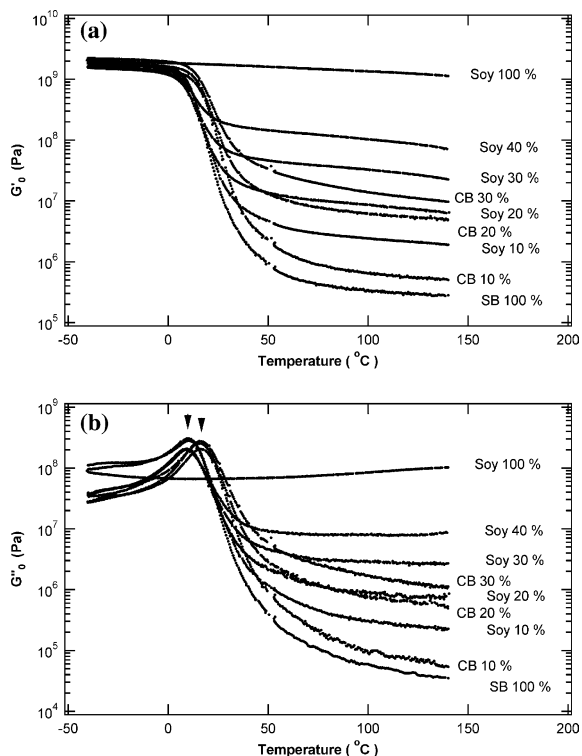


Fig. 1. (a) Storage modulus of Soy/SB and CB/SB composites (b) Loss modulus of Soy/SB and CB/SB composites. The weight fraction of filler is indicated at the end of each curve.

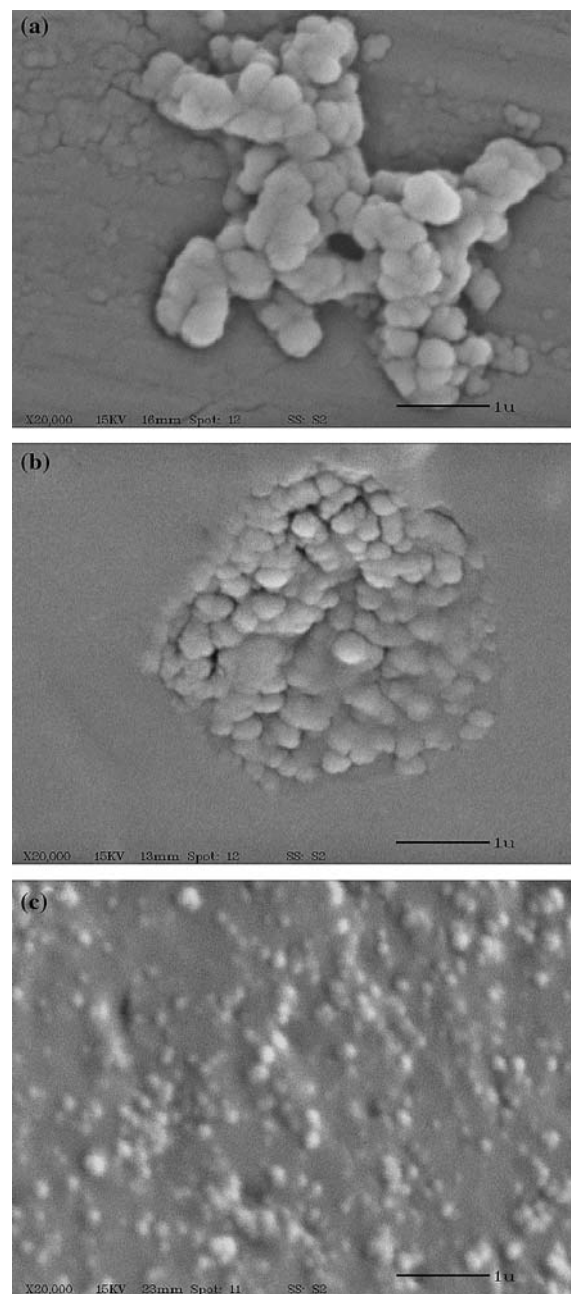


Fig. 2. (a) A soy protein aggregate on an aluminum substrate (b) Soy protein aggregates embedded in the fractured surface of a 40/60 Soy/SB composite (c) CB aggregates embedded in the fractured surface of a 30/70 CB/SB composite. The black scale bar shown is 1 micron.

and ionic bonding. From Fig. 1b, an upward shifting of approximately 5°C in the position of loss maxima of the carbon black composites was observed, but not in the protein composites. The

loss maxima of protein composites are at $\sim 11^\circ\text{C}$ and are very close to the glass transition temperature of $\sim 10^\circ\text{C}$ measured by DSC. This can be explained from the aggregate size of these two types of fillers. Some of the smaller aggregates of carbon black can act as crosslinking points and therefore cause a slight increase in the effective crosslinking density of the rubber. Such increase in glass transition temperature, however, is also an indication of the smaller size of carbon black aggregates produced by the current high shear process. For carbon black prepared by conventional compounding process, the shifting of T_g is usually not observed [16]. For the protein clusters, the size is larger and act only as filler without affecting the effective crosslinking density of the rubber.

Another difference between protein and carbon black is that the elastic modulus of carbon black composites decreases more rapidly with increasing temperature, while that of the protein composites tends to decrease slowly with temperature then reaches a plateau value. This is an interesting indication that the strength of filler network structures of these two types of fillers in the composites is different. This also indicates the soy protein network has a better high temperature stability, while the network structures of carbon black are more significantly weakened by the increasing temperature. For a comparison at the same volume fraction, the elastic modulus versus volume fraction is shown in Fig. 3. Protein composites have a slightly higher elastic modulus at the same volume fraction of filler. Since CB has smaller aggregate size than that of protein, the effective volume fraction of CB is greater than that of protein assuming the filler–rubber interaction is the same. The effective volume fraction of CB can further increase if the CB–rubber interaction is stronger than that of protein. A greater volume fraction of immobilized rubber in CB composites should yield a better stability at the higher temperatures, but the opposite was observed when compared to the protein composites. The fact that the shear elastic moduli of protein composites at the small strain region are more stable at the higher temperatures indicates the protein network strength is a dominant factor and outweighs the effect of filler–rubber interaction. This interpretation is consistent with the recovery behavior of protein composites that will be discussed later. To examine if the surfactant modification of carbon black surface has any effect on the inter-cluster interaction as the temperature

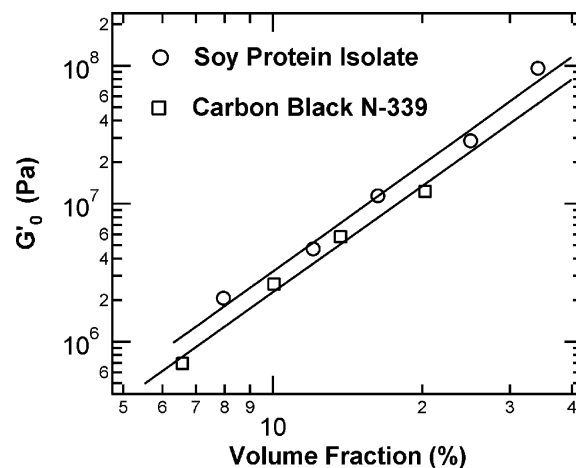


Fig. 3. Shear elastic modulus of Soy/SB and CB/SB composites at different volume fractions measured at 140°C . G'_0 is the elastic modulus at linear viscoelastic region.

increases, the G' decay rate of the CB composite with temperature is compared with that of other traditionally compounded carbon black/rubber composites [16, 24] by superimposing the transition zone. It was found the decay rates with temperature are similar among these cases with similar carbon black content (~ 30 wt%). This indicates the surfactant used in the preparation of carbon black dispersion does not have a significant effect on the temperature behavior.

Stress Softening Effect

Stress softening effect occurs in most filled elastomers. The effect is defined as the reduction of stress required to deform the filled rubber at a given elongation during the second cycle of deformation. The effect is also called Mullin effect for his extensive studies [25, 26] on this phenomenon. Stress softening effect is generally accepted as originated from the filler-related structures and therefore can yield some insight into the filler structures [16]. The stress softening effect of 100% styrene–butadiene (SB) rubber, 30% soy protein-filled styrene–butadiene rubber composite (30/70 Soy/SB), and 30% carbon black-filled styrene–butadiene rubber composite (30/70 CB/SB) are shown in Fig. 3. Similar to carbon black or silica-filled elastomers [16], the protein composites show a significant reduction of shear elastic moduli after the first strain cycle.

At 80°C , the strain sweep curves for both 30/70 Soy/SB and CB/SB composites become reproducible

after three cycles of dynamic strain. 100% styrene–butadiene rubber also shows stress softening effect, but its contribution to the stress softening effect of the composites is not significant. This is evident by comparing the difference between the shear elastic modulus of the first and the eighth strain cycle in Fig. 4a, b. The contribution of stress softening effect from the rubber is less than 0.5% in the stress softening effect of 30/70 Soy/SB or 30/70 CB/SB composite. The stress softening effect in protein/rubber composites is mostly from the contribution of the protein-related structures such as protein network and protein–rubber interactions. The increasing magnitude of strain (deformation) in the first three strain cycles obviously causes the protein network to break down and possibly the polymer chains to detach from the protein aggregates. In this aspect, the current protein/rubber composites are not very different from the well-known carbon black-filled rubber composites. After three strain cycles, protein-related network structures can be weakened and rebuilt and is an indication of reaching an equilibrium condition. For loss modulus, the energy dissipation process becomes less pronounced and the maxima are shifted to the lower strain amplitudes. The structure responsible for the energy dissipation process is

obviously reduced after the first three cycles. Comparing the protein composite with the carbon black-filled composite, the magnitude of loss maximum in the protein composite is not as pronounced as that in the carbon black composite.

The magnitudes of shifting in the position of loss maxima in Fig. 4b, c are different. At 80°C, the Soy/SB composite in Fig. 4b exhibits a loss maximum at 1.2% strain in the first cycle, while CB/SB composite in Fig. 4c has a loss maximum at 0.98% strain in the first cycle. This may indicate the protein network and related structures are stronger and can only be weakened at a larger strain. In the eighth cycle, the loss maximum of protein composite occurs at 0.31% strain and that of the carbon black composite is at 0.59% strain. A greater shifting of loss maximum towards the lower strain at the eighth cycle in the protein composite may indicate the protein-related network structure is slower to recover than that of the CB composite within the same period. This is not an effect of filler volume fraction. As shown in Fig. 5, 20/80 Soy/SB composite has a smaller filler volume fraction than that of 30/70 CB/SB composite and yet exhibits the same tendency. At 140°C, the same phenomenon was again observed in Fig. 6. This observation is also consistent with the recov-

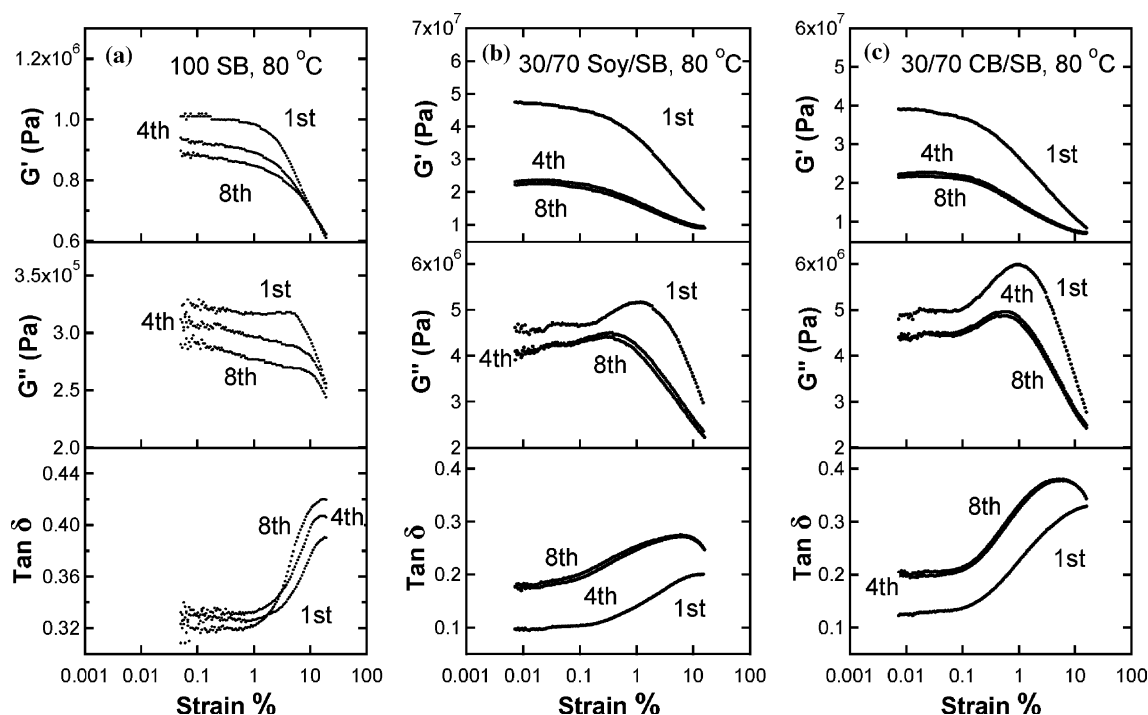


Fig. 4. Strain sweep experiments: (a) 100% SB at 80°C (b) 30/70 Soy/SB composite at 80°C (c) 30/70 CB/SB composite at 80°C.

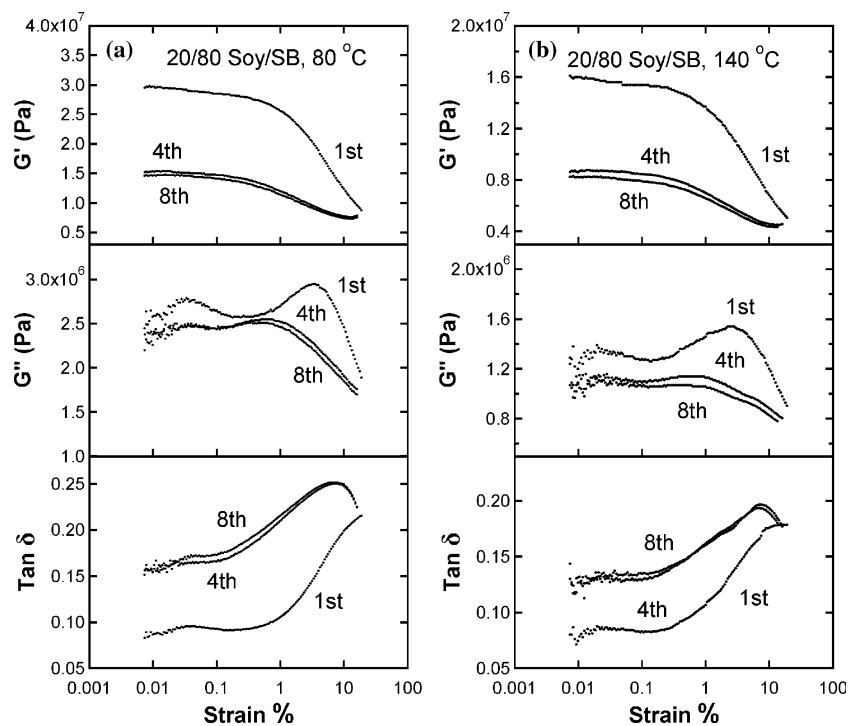


Fig. 5. Strain sweep experiments: (a) 20/80 Soy/SB composite at 80°C (b) 20/80 Soy/SB composite at 140°C.

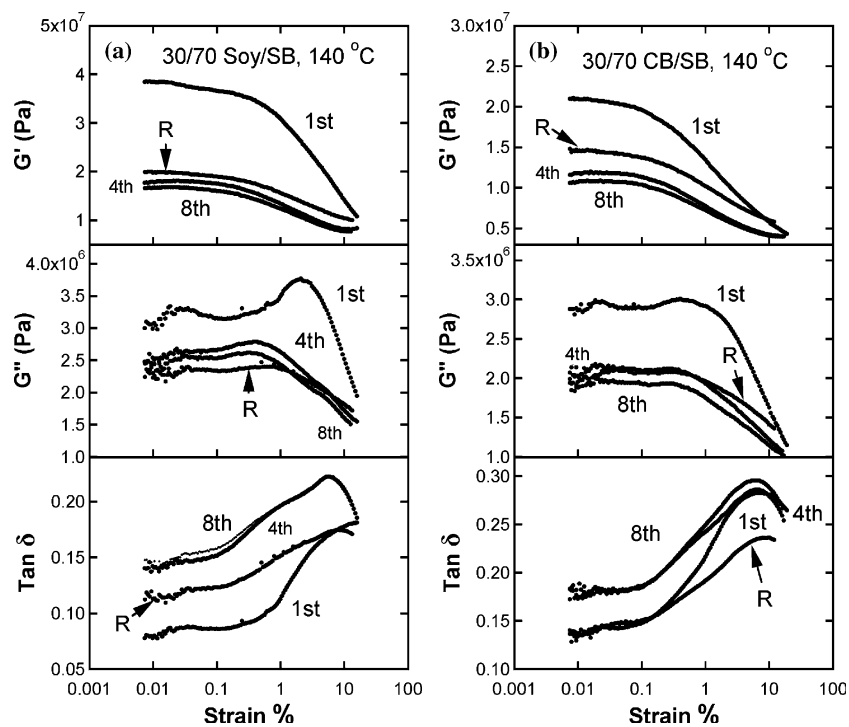


Fig. 6. Strain sweep experiments: (a) 30/70 Soy/SB composite at 140°C (b) 30/70 CB/SB composite at 140°C. R is the recovery curve after the samples are conditioned at ambient temperature for 147 days and 140°C for 1 day.

ery curves shown in Fig. 6a and b, which indicates the CB composite has a better recovery in the modulus values than that of the protein composite under the same condition. A stronger filler–rubber interaction in the CB composites compared to that of the soy protein can explain these recovery behaviors [27]. The protein–rubber interaction in the composites is a subject of further study by solid state NMR.

At a higher temperature of 140°C, the loss maxima shown in Fig. 6 are just the opposite of that in Fig. 4. The loss maximum in 30/70 Soy/SB composite is more pronounced than that in 30/70 CB/SB composites. This is consistent with the high temperature behavior of carbon black composites shown in Fig. 1. The carbon black-related structure is more significantly weakened by the high temperature effect. Only a fraction of this structure remains strong enough to be weakened and rebuilt under the effect of dynamic strain. On the other hand, the protein-related network structure is not significantly affected by the high temperature and most filler related structures remain to be weakened and rebuilt under the dynamic strain.

Payne Effect

In order to understand the reinforcement effect of soy protein isolate, the composites were subjected to oscillatory strain at different magnitude similar to the previous stress softening effect. The shear elastic moduli of filled elastomers with 10, 20, and 30% of soy protein aggregates are shown in Fig. 7. A composite with 30% CB is also shown in Fig. 7d for comparison. The data shown is the eighth cycle of strain sweep. The resulting modulus-strain spectra are very similar to that of carbon black [16]. The reduction of shear elastic modulus with increasing strain is a familiar phenomenon reported in the early 1960's by Payne on carbon black-filled rubbers. Later, Kraus [28] based on Payne's idea of filler networking proposed a phenomenological model. The model is based on the aggregation and de-aggregation of carbon black agglomerates. In this model, the carbon black contacts are continuously broken and reformed under a periodic sinusoidal strain. Based on this kinetic aggregate forming and breaking mechanism at equilibrium, elastic modulus was expressed as follows.

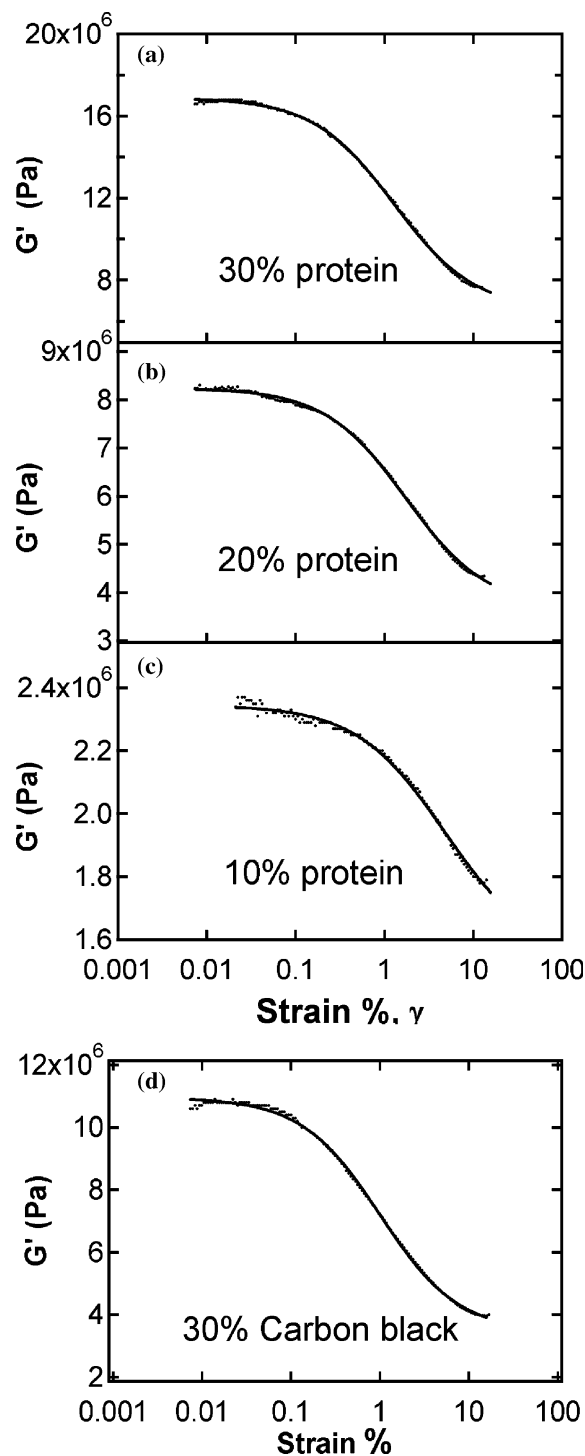


Fig. 7. The eighth cycle of strain sweep experiments at 140°C and 1 Hz. (a) 30/70 Soy/SB composite (b) 20/80 Soy/SB composite (c) 10/90 Soy/SB composite (d) 30/70 CB/SB composite. Solid lines are the fit from Kraus model.

$$\frac{G'(\gamma) - G'_\infty}{G'_0 - G'_\infty} = \frac{1}{1 + (\gamma/\gamma_c)^{2m}} \quad (1)$$

where, G'_∞ is equal to $G'(\gamma)$ at very large strain and G'_0 is equal to $G'(\gamma)$ at very small strain. γ_c is a characteristic strain where $G'_0 - G'_\infty$ is reduced to half of its zero-strain value. m is a fitting parameter related to filler aggregate structures. Equation (1) has been shown to describe the behavior of $G'(\gamma)$ in carbon black-filled rubber reasonably [15]. The loss modulus and loss tangent, however, do not have a good agreement with experiments [29], mainly due to the uncertainty in the formulation of loss mechanism. Recently, Huber et al. also modeled Payne effect and gave a similar expression as Kraus model, but with a physical interpretation of the fitting parameter m in Kraus model. Based on the cluster-cluster aggregation (CCA) model, Huber et al. [30] obtained $m = 1/(C - d_f + 2)$, where C is a connectivity exponent related to the minimum path along the cluster structure and d_f is the fractal dimension of clusters. C is ~ 1.3 in CCA model. Previously, the fractal dimension of protein clusters was estimated to be 1.3 to 1.5 [23]. m can be calculated from the fractal dimension of soy protein and is listed in Table I along with other fitting parameters. The agreement between the calculation and the best fit of experimental data shown in Fig. 7 is reasonable. $m \sim 0.44$ for 10/90 Soy/SB composite is slightly lower than that for the 20/80 and 30/70 Soy/SB composites. This can be attributed to a more scattered data at small strain region as shown in Fig. 7c. In this model comparison, the uncertainty in the factor C has to be considered. For the protein clusters, C is not measured and can vary from 1 to d_f according to the strong-link model [31]. If one allows C to vary from 1 to d_f , m will vary

from 0.5 to 0.6. For the soy protein composites, $m \sim 0.5$ is close to the lower limit in this model. For the 30% carbon black filled elastomer, the fractal dimension of carbon black aggregates can be estimated from the slope of G'_0 shown in Fig. 2. The estimated fractal dimension is 1.31–1.44 by using strong-link model. m calculated from the estimated fractal dimension is also listed in Table I for comparison. $m \sim 0.5$ is about the same as that of soy protein composites and is also consistent with literature values, $m = 0.5 - 0.6$ [15, 32, 33]. The result in Table I indicates soy protein aggregates also forms a filler related network similar to carbon black aggregates in rubbers. From the recovery behaviors in the stress softening effect and the fitting results of Kraus model, the kinetic aggregation and de-aggregation mechanism perhaps should be more appropriately described as the elasticity of protein immobilized rubber structured by the surface area and fractal dimension of protein aggregates.

CONCLUSIONS

Soy protein isolate was incorporated at different levels into carboxylated SB elastomers. In the rubber plateau region, a very significant increase in the equilibrium storage modulus of dry composites was observed when compared with that of 100% carboxylated SB elastomer. The observed significant reinforcement effect was studied by dynamic temperature sweep experiments and compared with carbon black/rubber composites. At the same weight fraction of fillers, dry soy protein aggregates exhibit a higher reinforcement effect than that of carbon black in the rubber plateau region and their moduli are less sensitive to the higher temperatures. The protein composites are also studied by the dynamic strain sweep experiments to understand the filler related

Table I. Fit Parameters of Shear Elastic Modulus^a

| Composition soy/SB | Best fit ^b (m) | | Calculated ^c (m) | γ_c (%) 8th cycle | G'_0 (MPa) 8th cycle | G'_∞ (MPa) 8th cycle |
|--------------------|-------------------------------|-----------|---------------------------------|--------------------------|------------------------|-----------------------------|
| | 4th cycle | 8th cycle | | | | |
| 10/90 | 0.46 | 0.44 | 0.51 | 4.75 | 2.35 | 1.54 |
| 20/80 | 0.52 | 0.48 | 0.51 | 1.74 | 8.24 | 3.68 |
| 30/70 | 0.52 | 0.48 | 0.51 | 1.29 | 16.9 | 6.55 |
| CB/SB | | | | | | |
| 30/70 | 0.50 | 0.49 | 0.5–0.54 | 1.00 | 11.0 | 3.45 |

^a Measured at 140°C.

^b Best fit of shear elastic modulus versus strain with Kraus Model.

^c Calculated from $m = 1/(C - d_f + 2)$, $C = 1.3$ in CCA model.

structures. The soy protein-related network structure exhibits similar behavior to that of carbon black in terms of reversible structure breakdown after 3 cycles of dynamic shear strain. However, carbon black composites show a better recovery behavior after eight cycles of dynamic strain. The Payne effect of protein composites at 140°C was interpreted using the Kraus model. The fitting parameter m was interpreted with Huber–Vigil's expression and related to the fractal structure of the soy protein aggregates. The agreement between the theoretical model and the experiments is reasonable. From the comparison with CCA model, the reinforcement effect of soy protein can be reasonably described by the kinetic cluster–cluster aggregation mechanism of protein-related structures.

ACKNOWLEDGMENTS

The author thanks Dr. A. R. Thompson for scanning electron microscopy and A. J. Thomas for the help on the instrumentation.

REFERENCES

1. H. Ismail, R. M. Jaffri, and H. D. Rozman (2003) *J. Elastomers Plast.* **35**(2), 181–192.
2. K. G. Nair and A. Dufresne (2003) *Biomacromolecules*, **4**, 666–674.
3. H. Ismail, S. Shuhelmy, and M. R. Edyham (2001) *Eur. Polym. J.* **38**(1), 39–47.
4. C. Wang and C. J. Carriere (2001) *U.S. Patent* 6,310,136 B1.
5. S. Wang, H. J. Sue, and J. Jane (1996) *J M S-Pure Appl. Chem. A*, **33**(5), 557–569.
6. J. John and M. Bhattacharya (1999) *Polym Int.* **48**, 1165–1172.
7. X. Mo, X. S. Sun, and Y. Wang (1999) *J. Appl. Polym. Sci.* **73**, 2595–2602.
8. Q. Wu and L. Zhand (2001) *Ind. Eng. Chem. Res.* **40**, 1879–1883.
9. E. T. A. Coughlin (1936) *U.S. Patent* 2,056,958.
10. M. R. Isaacs (1938) *U.S. Patent* 2,127,298.
11. R. L. Lehmann, B. J. Petusseau, and C. P. Pinazzi (1960) *U.S. Patent* 2,931,845.
12. C. T. Fuetterer (1963) *U.S. Patent* 3,113,605.
13. O. Beckmann, R. Teves, and W. Loreth (1996) *Ger. Offen. DE* 19622169 A1 19961212.
14. C. Recker (2002) *Eur. Pat. Appl.* EP 1234852 A1 20020828.
15. G. Heinrich and M. Kluppel (2002) *Adv. Polym. Sci.* **160**, 1–44.
16. M. J. Wang (1998) *Rubber Chem. Technol.* **71**, 520–589.
17. M. C. Garcia, M. Torre, M. L. Marina, and F. Laborda (1997) *Crit. Rev. Food Sci. Nutr.* **37**(4), 361–391.
18. J. Richard (1992) *Polymer*, **33**, 562–571.
19. A. Zosel and G. Ley (1993) *Macromolecules*, **26**, 2222–2227.
20. C. S. Kan and J. H. Blackson (1996) *Macromolecules* **29**, 6853–6864.
21. X. Li, X. Liu, and H. Xie (2000) *Tanxingti*, **10**(4), 21–24.
22. L. Chazeau, J. D. Brown, L. C. Yanyo, and S. S. Sternstein (2000) *Polym. Compos.* **21**, 202–222.
23. L. Jong (2004) *Polym. Mater. Sci. Eng.* **90**, 769–770.
24. H. S. Y. Hsieh, L. C. Yanyo, and R. J. Ambrose (1984) *J. Appl. Polym. Sci.* **29**, 413–425.
25. L. Mullins (1947) *J. Rubber. Res.* **16**, 275–289.
26. L. Mullins (1950) *Phys. Colloid Chem.* **54**, 239–251.
27. A. Zhu and S. S. Sternstein (2003) *Compos. Sci. Technol.* **63**, 1113–1126.
28. G. Kraus (1984) *J. Appl. Polym. Sci., Appl. Polym. Symp.* **39**, 75–92.
29. J. D. Ulmer (1995) *Rubber Chem. Technol.* **69**, 15–47.
30. G. Huber and T. A. Vilgis (1999) *Kautsch. Gummi. Kunstst.* **52**, 102–107.
31. W. Shih, W. Y. Shih, S. Kim, J. Liu, and I. A. Aksay (1990) *Phys. Rev. A*, **42**, 4772–4779.
32. G. Heinrich and T. A. Vilgis (1995) *Macromol. Chem. Phys., Macromol. Symp.* **93**, 253–260.
33. S. Vieweg, R. Unger, K. Schroter, E. Donth, and G. Heinrich (1995) *Polym. Networks Blends*, **5**, 199–204.